Ratcheting and fatigue behavior of Eurofer97 at high temperature, part 1: experiment

Kuo Zhang[1,2], Mario Walter[1], Jarir Aktaa[1]

[1]Karlsruhe Institute of Technology, Institute for Applied Materials, Hermann-von-Helmholtz-Platz 1, 76344 Eggenstein-Leopoldshafen, Germany

[2]Max Planck Institute of Plasma Physics, Boltzmannstraße 2, 85748 Garching, Germany

Abstract

Eurofer97 is considered as one of the structural material candidates for in-vessel components of future fusion reactor. Due to frequent startups, shutdowns and load changes in reactor, the material is under complex cyclic loadings. This work investigates the mechanical behavior of Eurofer97 under various cyclic loadings, including strain-controlled LCF tests and stress-controlled ratcheting tests at high temperatures 450°C and 550°C. Various influencing factors on ratcheting, such as stress magnitude, stress ratio and stress rate are evaluated. Since Eurofer97 is developed based on conventional grade 91 ferritic martensitic (FM) steels, corresponding data of mod.9Cr-1Mo FM steel P91 are also presented for comparison.

Key Words

Eurofer97; Cyclic loading; 450°C and 550°C

1. Introduction

Eurofer97 belongs to the group of Reduced-Activation Ferritic-Martensitic (RAFM) steels. The RAFM steels are designed as structural materials for first wall and blanket systems of future fusion power plant [1-3]. Comparing to conventional grade 91 ferritic-martensitic (FM) steels, such as P91, highly radioactive elements are replaced (Mo by W, Nb by Ta) or minimized [4-8].

The working conditions of structural materials such as Eurofer97 in reactor usually include frequent startups, shutdowns and load changes which lead to complex thermo-mechanical loading and different mechanical damages [2]. Under cyclic asymmetric loading, the mean strain accumulates in the direction of mean stress, which is referred to as “ratcheting behavior”.

One of the earliest observations of ratcheting was reported for 1100 aluminum, which showed shifting of hysteresis loops in the presence of mean stress [9]. Researchers have found ratcheting effect on a wide range of materials, including:

- Austenitic steels such as 316L [10-12], 316LN [13], 304 [14-21], 304L [22], 304LN [23]
- Ferritic steels [24-28];
- Carbon steels (CS) 40Cr [29], 42CrMo [19, 30, 31], 16MnR[32], X42 and X56 [33], 20 CS [34, 35], 45 CS [36];
- Other steels such as SA333C–Mn steels [37], Interstitial-Free Steel [38];
- Other metallic materials, such as zirconium alloys [39], pure titanium [40], titanium alloys [41], NiTi shape memory alloy [42, 43];
- Ceramic matrix composites [44];
- Polymers such as polytetrafluoroethylenes (PTFE) [45], polypropylene [46], polyacetal/polyoxymethylene[47], epoxy resin[48].

Generally speaking, ratcheting happens with a non-zero mean stress, or in other words, asymmetric stress-controlled loading. A phenomenon named “dynamic strain aging” was found for austenitic steel 304 in the temperature range of 400–600 °C [16]. The explanation for this phenomenon was that the interactions of dislocation and point defect were significantly active, which resulted in a remarkable enhancement of deformation resistance, hence the cyclic hardening was greater.

Although ratcheting tests are supposed to be performed under stress-controlled cyclic loading, strain-controlled ratcheting tests were also performed on austenitic steel 316L at RT and 200 °C [10, 11], which are known as “cyclic tension tests”. It was suggested that the material response was a superposition of two mechanisms: a cyclic one (hardening corresponding to LCF behavior) and a monotonic one (hardening owing to drifting of the mean strain).

Compared to austenitic steels, ratcheting research on ferritic steels is relatively sparse. The ratcheting behaviors of grade 91 FM steels have been previously reported [26, 49, 50]. On the other hand, cyclic softening of grade 91 FM steels as well as Eurofer97 have been observed in low cycle fatigue tests [2, 24, 26, 50]. Besides, fatigue crack is also one of the mechanical damages under cyclic loading. All these phenomena shall be considered in the design of construction rules for the structural materials in reactor.

This report focuses on the ratcheting behavior of Eurofer97 at 450°C and 550°C. Since ratcheting behavior at 550°C has been already reported in the previous paper[51], this report presents new testing results at 450°C and compares with the data at 550°C. Material properties of mod.9Cr-1Mo FM steel (P91) are also presented to compare with those of Eurofer97.

2. Material and testing

In this research, mechanical behavior of Eurofer97 batch 2 specimens is investigated, both in strain-controlled and stress-controlled low cycle fatigue tests. The material is normalized at 980°C for 30min and tempered at 760°C for 90min. The specimens are firstly cut by electrical discharge machining (EDM) and further turned and polished to nominal diameter of 8.8mm and gauge length of 23mm.

	Eurofer97 specified (wt%)	Mod. 9Cr-1Mo FM steel (P91) measrued (wt%)
C	0.09 – 0.12 [0.11]	0.086
Cr	8.5 – 9.5 [9.0]	8.910
W	1.0 – 1.2 [1.1]	0.01
Ta	0.10 – 0.14 [0.12]	/
Mn	0.20 – 0.60 [0.40]	0.363
V	0.15 – 0.25	0.198
N_2	0.015 – 0.045 [0.030]	0.041
P	<0.005	0.017
S	<0.005	0.001
B	<0.001	0.001
O_2	<0.01	0.002
Mo	<0.005	0.917
Nb	<0.001	0.08
Ni	<0.005	0.149
Cu	<0.005	0.068
Al	<0.01	0.018
Si	<0.05	0.324
Ti	<0.01	0.002
Co	<0.005	/

Table 1 Specification of chemical compositions of Eurofer97 [50, 52]

The detailed specifications of the chemical compositions of Eurofer97 are listed in Table 1. The measured chemical compositions of P91 are also listed for comparison. It is clear that around 1 wt% of Mo is replaced by W and 0.08 wt% of Nb is replaced by 0.12 wt% of Ta. Elements such as P, Ni, Cu, Al etc. are minimized; while wt% of Cr and C are kept to around 9% and 0.1%, respectively.

The chemical compositions of Eurofer97 batch 2 follow the same specification of batch 1. However batch 1 is produced in a way of massive industrial production. Note that the fatigue behavior in the previous report[2] is of Eurofer97 batch 1. The current paper presents data of batch 2, if not mentioned otherwise.

Strain-controlled low cycle fatigue (LCF) tests are performed at 450°C and 550°C. The total strains $\Delta\varepsilon$ range between 0.4% and 1.5%. At 550°C, LCF tests are performed with the strain rate $3 \times 10^{-3}\ 1/s$. At 450°C, LCF tests are performed with the strain rate $3 \times 10^{-4}\ 1/s$. The mean strain is kept at zero.

Stress-controlled uniaxial ratcheting tests are performed with the same type of specimens, also at 450°C and 550°C. The test matrix for 450°C and 550°C is presented in Table 2 and Table 3, respectively.

a) Influence of peak stress

σ_{max} [MPa]	425	400	380	365	350	325
σ_{min} [MPa]	-382.5	-360	-342	-328.5	-315	-292.5
Stress ratio	-0.9					
σ_{mean} [MPa]	21.25	20	19	18.25	17.5	16.25
$\dot{\sigma}$[MPa/s]	±50					

b) Influence of mean stress/stress ratio

σ_{max} [MPa]	380							
σ_{min} [MPa]	0	-190	266	-304	-342	-361	-372.4	-380
Stress ratio	0.0	-0.5	-0.7	-0.8	-0.9	-0.95	-0.98	-1.0
σ_{mean} [MPa]	190	95	57	38	19	9.5	3.8	0
$\dot{\sigma}$ [MPa/s]	±50							

c) Influence of stress rate

σ_{max} [MPa]	380		
σ_{min} [MPa]	-342		
$\dot{\sigma}$ [MPa/s]	±10	±50	±250

Table 2 Stress-controlled uniaxial tests on Eurofer97 at 450°C

a) Influence of peak stress

σ_{max} [MPa]	350	335	325	315	300	285	265	250
σ_{min} [MPa]	-315	-301.5	-292.5	-283.5	-270	-256.5	-238.5	-225
Stress ratio	-0.9							
σ_{mean} [MPa]	17.5	16.75	16.25	15.75	15	14.25	13.25	12.5
$\dot{\sigma}$[MPa/s]	±50							

b) Influence of mean stress/stress ratio

σ_{max} [MPa]	300							
σ_{min} [MPa]	0	-150	210	-240	-270	-285	-294	-300
Stress ratio	0.0	-0.5	-0.7	-0.8	-0.9	-0.95	-0.98	-1.0
σ_{mean} [MPa]	150	75	45	30	15	7.5	3	0
$\dot{\sigma}$ [MPa/s]	±50							

c) Influence of stress rate

σ_{max} [MPa]	300		
σ_{min} [MPa]	-270		
$\dot{\sigma}$ [MPa/s]	±10	±50	±250

Table 3 Stress-controlled uniaxial tests on Eurofer97 at 550°C

As shown in Table 2 and Table 3, for each temperature, the tests are in three groups: group a) includes tests with the same stress ratio. The peak stress varies in a range of 100MPa. The stress rate for all test is 50MPa/s. According to previous study on the ratcheting behavior of P91 at room temperature and 550°C [50], the highest ratcheting rate appears at a stress ratio between -1 and -0.9, it is therefore more reasonable to keep the stress ratio instead of keeping the mean stress constant, to find the approximately highest ratcheting rate for each peak stress.

Group b) includes tests with the same peak stress and stress rate. The stress ratios range from -1 to 0, in another word, the loading condition varies between symmetric loading to monotonic tensile loading.

Group c) includes tests with the same peak stress and stress ratio, but three different stress rates. These tests reveal the visco-plasticity of the material.

Note that the stress-controlled ratcheting tests are performed with true-stress-controlling, since for instance, 3% of accumulated strain leads to 3% difference between true- and engineering stress, which is already too large. Further, the results from the true-stress-controlled tests are relatively simpler to be interpreted for building and fitting a suitable material model.

3. Experimental results

3.1 Strain-controlled LCF tests

Experimental results of the strain-controlled LCF tests are illustrated in Figure 1.

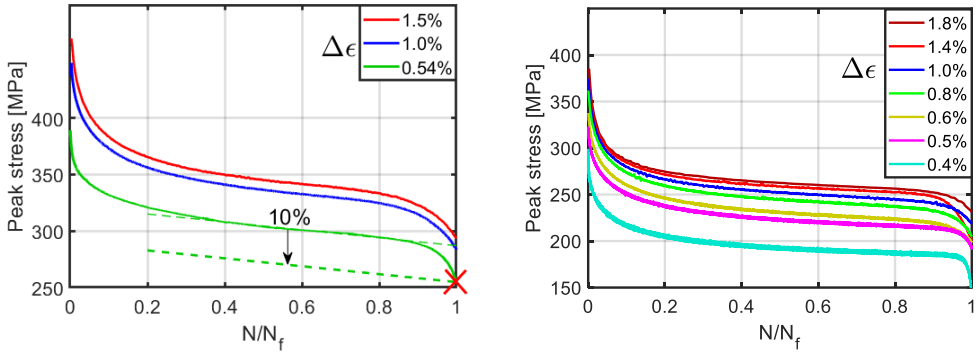

a) b)

Figure 1. Peak stresses vs. normalized number of cycles in strain-controlled LCF tests. a) 450°C. b) 550°C.

Figure 1 shows the peak stresses versus the normalized number of cycles, by dividing the cycle number with the number of cycles to failure. Clear cyclic softening at both testing temperatures is shown. The peak stresses decrease rapidly until around 20% of life time, and then they decrease linearly and smoothly until around 80% of life time. This second stage is also called saturation stage, followed by again rapid decrease due to fatigue crack growth.

The number of cycles to failure is defined at the cycle where the peak stress has decreased by 10% from that predicted by the extrapolation of the saturation curve, as by Saad et al.[53]. This method is shown in Figure 1. a) for $\Delta\varepsilon = 0.54\%$ as an example. The red cross marks the end of the fatigue lives.

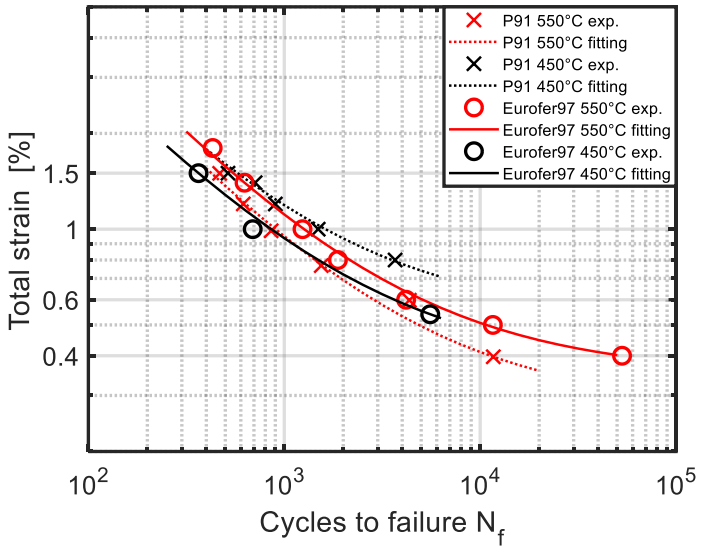

Figure 2. Total strains vs. numbers of cycles to failure with fittings.

Fittings are performed for the relationship between total strains and the number of cycles to failure, both for 450°C and 550°C following the form $\Delta\varepsilon = a_1 + a_2 N_f^{a_3}$ in [54]. Corresponding values of P91 are also presented for comparison. The fittings are shown in Figure 2. The resulting fitting equations are as follows:

P91 550°C: $\Delta\varepsilon = 2.746 \times 10^{-3} + 0.8218 \times {N_f}^{-0.69505}$

P91 450°C: $\Delta\varepsilon = 5.208 \times 10^{-3} + 0.7985 \times {N_f}^{-0.6922}$

Eurofer97 550°C: $\Delta\varepsilon = 3.757 \times 10^{-3} + 1.9696 \times {N_f}^{-0.6841}$

Eurofer97 450°C: $\Delta\varepsilon = 3.578 \times 10^{-3} + 0.6089 \times {N_f}^{-0.6739}$

It is curious that the fatigue lives of Eurofer97 at 450°C are shorter than at 550°C, though marginally, while it is the other way around for P91. For more information, literature data of Eurofer97 have been collected and shown in Figure 3. Comparing FZK data at 450°C and 550°C of Eurofer97 batch 1, the fatigue lives at 450°C are marginally longer than at 550°C. However the fatigue data of batch 1 scatter too much to have a clear conclusion.

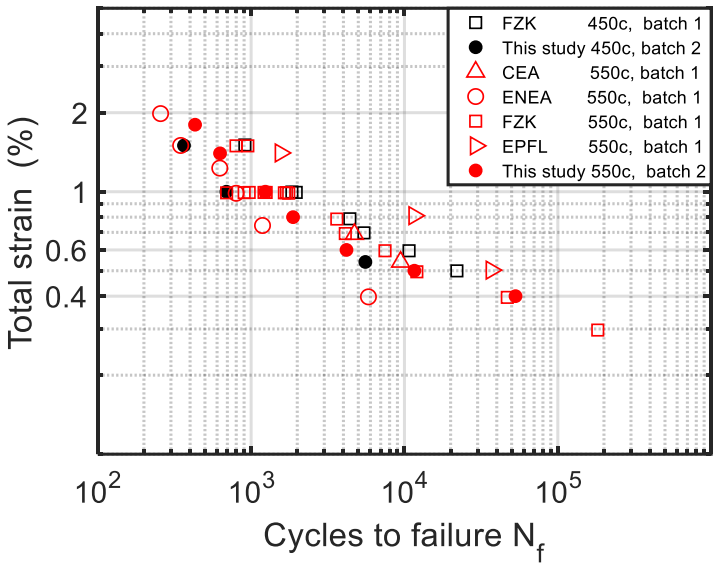

Figure 3 Fatigue life in LCF tests of Eurofer97.[54, 55]

The peak stresses at half-life time ($N/N_f = 0.5$) of Eurofer97 and P91 are shown in Figure 4. The induced peak stresses of Eurofer97 at 450°C are around 80MPa higher than those of Eurofer97 at 550°C. And the stresses of P91 at 550°C are around 40MPa higher than those of Eurofer97 at 550°C. The above information partly explains the different fatigue lives in Figure 2: The fatigue lives of Eurofer97 at 450°C are lower than those at 550°C due to higher induced stresses; The fatigue lives of P91 are lower than those of Eurofer97 at 550°C also due to higher induced stresses.

However the induced peak stresses of P91 at 450°C are higher than at 550°C, the difference goes from 69MPa to 97MPa, but P91 has inversely longer fatigue lives in LCF tests at 450°C than at 550°C. For further investigation, more LCF tests on Eurofer97 batch 2 are required, e.g. at more testing temperatures to evaluate the influence of temperature on low cycle fatigue behavior.

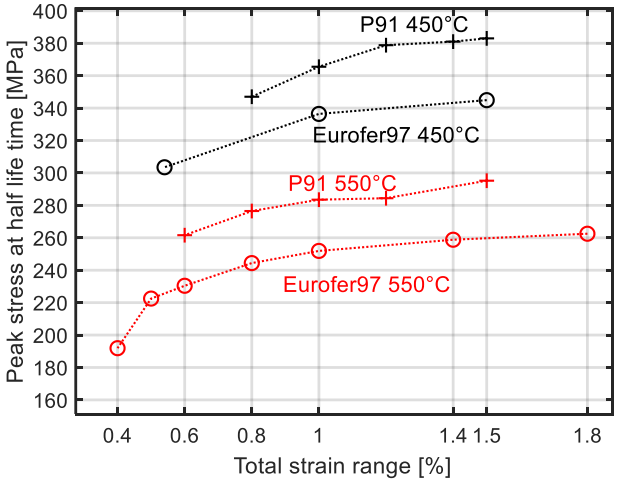

Figure 4 Peak stresses at half life time vs. total strain range in LCF tests.

3.2 Stress-controlled ratcheting tests

The test results under stress-controlling are shown in Figure 5-10.

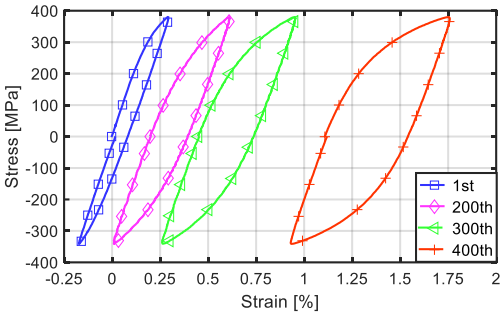

Figure 5. Stress-strain hysteresis loops of several loading cycles in the ratcheting test of Eurofer97 at 450°C, with max. stress = 380MPa, min. stress = -342MPa, stress rate = 50MPa/s.

Figure 5 shows the hysteresis loops of one of the ratcheting tests at 450°C for example. With a mean stress of 19MPa, the strain accumulates in the direction of this tensile mean stress. After around 400 loading cycles, the strain reaches over 1%, while the peak strain in the first loading cycle is only 0.3%. In spite of various magnitudes, this behavior is similar to the ratcheting behavior at 550°C which is reported in the previous work[51].

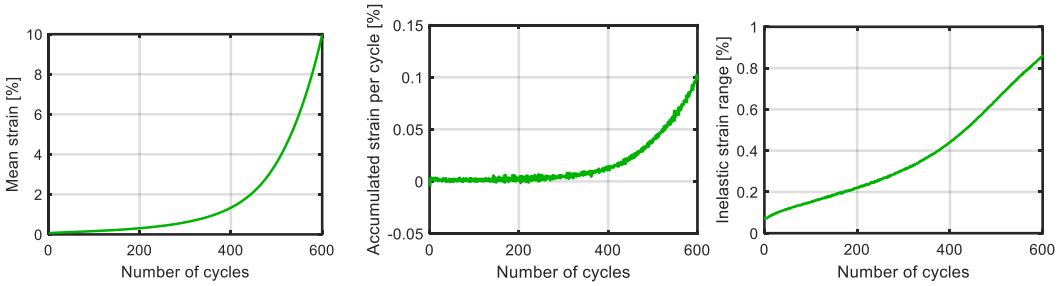

a) b) c)

Figure 6 Ratcheting test of Eurofer97 at 450°C with max. stress = 380MPa, min. stress = -342MPa, stress rate = 50MPa/s. a) Mean strain vs. cycle number. b) Accumulated strain per cycle vs. cycle number. c) Inelastic strain range vs. cycle number.

Figure 6 presents further analysis of the test as shown in Figure 5. Sub-Figure 6 a) shows the first impression of the ratcheting behavior: the mean strain accumulates with the increased cycle number. Sub-Figure 6 b) shows the accumulated strain per cycle, which is the rate of increase of a). And Sub-Figure 6 c) shows the inelastic strain range of each cycle.

These three sub-figures of Figure 6 indicate the cyclic softening of the material also under stress-controlled tests. However, comparing to the cyclic softening in strain-controlled LCF tests, shown in Figure 1, there is no distinction between rapid and saturated softening. It is because in strain-

controlled tests, the induced stress decreases significantly during the initial rapid softening stage, and becomes not sufficient for activating further rapid cyclic softening. While in stress-controlled cyclic loading, the stress is always high enough to activate cyclic softening. Hence, the rate of cyclic softening depends on the stress level.

It is found that, necking are observed on the Eurofer97 specimens after the accumulated strain reaches around 3%, as the same for steel P91 at 550°C [50]. Hence rapid increase of mean strain after it is over 3%, as shown in Figure 6 a), is mainly due to necking. And for this reason, 3% is chosen to be the critical percentage since no component should reach this total strain to avoid necking, as the same in [50].

Comparing the results from strain-controlled and stress-controlled cyclic tests, it is also found that, there is no macro fatigue crack appearing on any specimens in ratcheting tests. In order to find the reason, Figure 7 is shown as an example. The development of inelastic strain ranges in the two tests on Eurofer97 at 450°C are presented: one for the strain-controlled LCF test with total strain range 1%, the other one for the stress-controlled ratcheting test with stress alternating between 380 and -342MPa. According to Figure 1 and Figure 4, the stress range in the strain-controlled tests ($\Delta\varepsilon = 1\%$) is around 900MPa at the beginning, decreases to around 660MPa at half life time due to cyclic softening. While in the ratcheting test, the stress range is kept at 722MPa. As shown in Figure 7, the inelastic range in the strain-controlled test is initially much larger than that in the ratcheting test. Then the inelastic range of the ratcheting test catches up at around 500th cycle. Therefore, before 500th cycle, the microstructural development, e.g. crack initiation and micro crack propagation, due to inelastic strain in the strain-controlled test is always larger than that in this ratcheting test. However, the maximum strain at 500th cycle in this ratcheting test is already over 4%. This explains why there is no fatigue fracture of the tested ratcheting specimens. Hence, the ratcheting appears as a failure mode before the fatigue fracture takes place, since components such as those in e.g. piping systems should not exceed certain elongation.

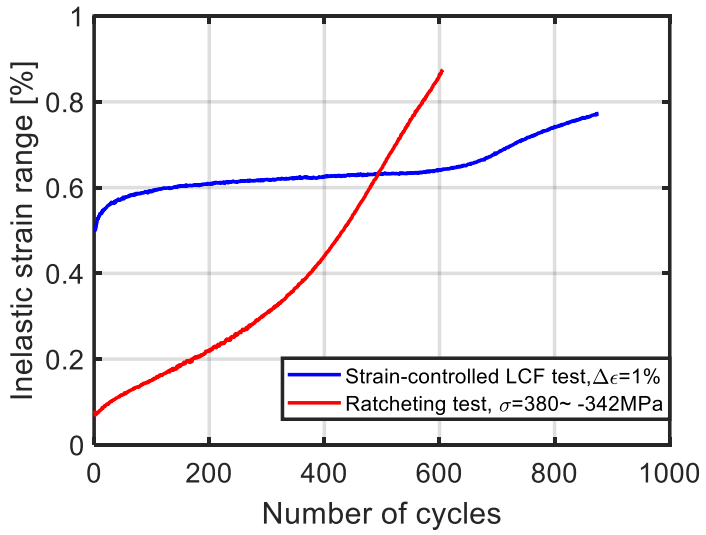

Figure 7 Inelastic strain ranges vs. number of cycles of strain- and stress-controlled test on Eurofer97 at 450°C.

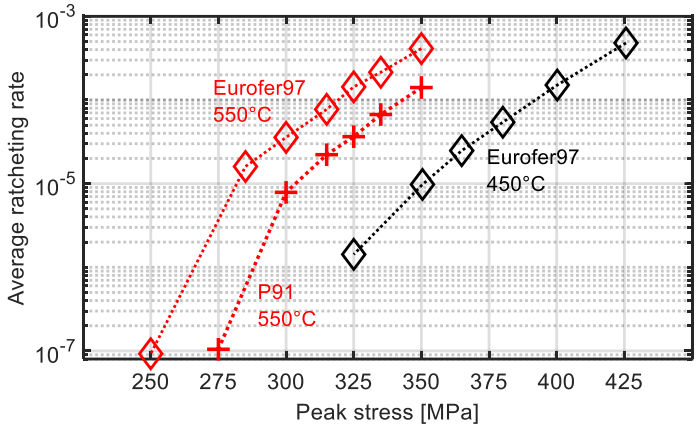

Figure 8. Average ratcheting rates vs. peak stresses with the stress ratio =-0.9 and stress rate = 50MPa/s [50, 51].

Tests with various peak stresses and the same stress ratio are performed at 450°C and 550°C according to Table 2 a) and Table 3 a). The average ratcheting rates until the accumulated strain reaches 3% or cycle number reaches 10,000 (whatever comes first) are shown in Figure 8. The average ratcheting rate is calculated as the mean strain divided by the corresponding cycle number.

The trends are obvious: higher peak stress leads to faster ratcheting.

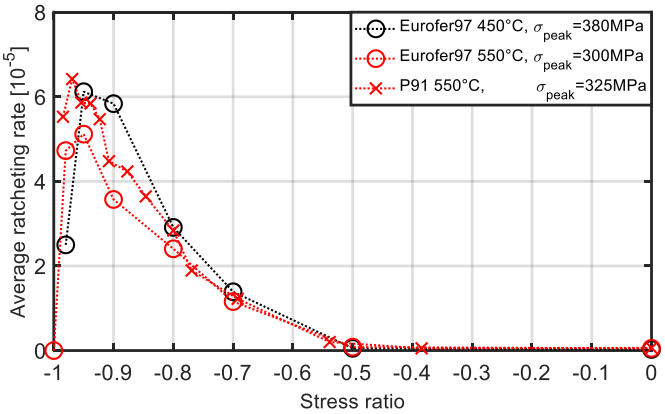

Figure 9 Average ratcheting rates vs. stress ratios with various stress ratios from -1 to 0 [50, 51].

Figure 9 presents the results of tests according to Table 2 b), Table 3 b) and the corresponding tests of P91 at 550°C. These tests are performed with the same peak stress and various stress ratios from -1 to 0. By choosing proper peak stress for each group of tests, the average ratcheting rates are comparable, to be shown in the same diagram. It is clear that the average ratcheting rates reach the maximum at a stress ratio between -1 and -0.9, for Eurofer97 at 450°C, 550°C and P91 at 550°C. With increase of stress ratio upto zero, the ratcheting rates decrease until becoming negligible.

The reason for the trend of the curves in Figure 9 is that, the lower stress ratio means larger stress range, which leads to larger inelastic strain.

First of all, ratcheting is a phenomenon of inelastic deformation. It is caused by the difference

between the changes of inelastic strains during the stress-increasing and stress-decreasing half in each loading cycle. These differences lead to non-closed hysteresis loops. And these differences accumulate cycle by cycle, leading to the ratcheting behavior. With larger stress range and lower stress ratio, both inelastic strains during the stress-increasing and -decreasing half are larger, and the inelastic strains during stress-increasing half is even larger than that during the stress-decreasing half in each loading cycle. Therefore, if stress ratio is within the range of 0 to around -0.9, the lower stress ratios lead to faster ratcheting. While increasing stress ratio upto zero, the loading tends into elastic range, therefore the ratcheting tends to becoming negligible.

On the other hand, the difference between the changes of inelastic strains during the stress-increasing and -decreasing halves reaches its maximum at a stress ratio between -1 and -0.9. When the stress ratio decreases further to -1, both inelastic strains (during the stress-increasing and -decreasing halves) enlarge further, however the difference in between decreases to zero. Hence, there is no ratcheting when the stress ratio is exactly -1, under the condition that the mechanical behavior under tension and compression is the same.

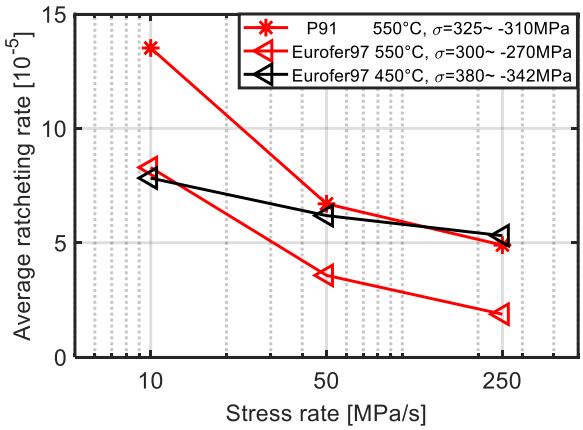

Figure 10 Average ratcheting rates vs. stress rates [50, 51].

Figure 10 shows the results according to Table 2 c), Table 3 c) with various stress rates (10, 50 and 250MPa/s) to investigate the visco-plasticity of the material. The data of Eurofer97 at 450°C and 550°C are shown, as well as data of P91 for comparison. The heights of the data points depend on the loading magnitudes. The inclination of each group of data points shows the influence of stress rate. It is clear that the visco-plasticity of P91 is similar to that of Eurofer97 at 550°C; while for Eurofer97 at 450°C, less visco-plasticity is observed due to lower temperature.

4. Conclusion

The mechanical behavior of Eurofer97 under isothermal uniaxial cyclic loading at 450°C and 550°C is investigated by performing strain-controlled and stress-controlled tests. The experimental data of mod.9Cr-1Mo FM steel P91 are compared with data of Eurofer97 at 550°C. It comes to the following conclusions: Although P91 is relatively tougher than Eurofer97, they share similar cyclic

softening and ratcheting behavior, including: a) Higher ratcheting rate with higher peak stress. b) Highest ratcheting rate with stress ratio between -1 and -0.9. c) Increasing ratcheting rate with decreasing stress rate. These findings are fully concordant with those of previous work [51] for Eurofer97 at 550°C.

Acknowledgement

This work is carried out within the R&D Nuclear Fusion Program of the Karlsruhe Institute of Technology (KIT).

References

[1] B. Raj and T. Jayakumar, "Development of Reduced Activation Ferritic–Martensitic Steels and fabrication technologies for Indian test blanket module", *Journal of Nuclear Materials,* vol. 417, pp. 72-76, 2011.

[2] J. Aktaa and R. Schmitt, "High temperature deformation and damage behavior of RAFM steels under low cycle fatigue loading: Experiments and modeling", *Fusion Engineering and Design,* vol. 81, pp. 2221-2231, 2006.

[3] V. B. Oliveira, H. R. Z. Sandim, and D. Raabe, "Abnormal grain growth in Eurofer-97 steel in the ferrite phase field", *Journal of Nuclear Materials,* vol. 485, pp. 23-38, 2017.

[4] C.-Y. Hsu and T. A. Lechtenberg, "Microstructure and mechanical properties of unirradiated low activation Ferritic steel", *Journal of Nuclear Materials,* vol. 141-143, Part2, pp. 1107-1112, 1986.

[5] R. L. Klueh and A. T. Nelson, "Ferritic/martensitic steels for next-generation reactors", *Journal of Nuclear Materials,* vol. 371, pp. 37-52, 2007.

[6] H. Kayano, H. Kurishita, A. Kimura, M. Narui, M. Yamazaki, and Y. Suzuki, "Charpy impact testing using miniature specimens and its application to the study of irradiation behavior of low-activation ferritic steels", *journal of Nuclear Materials,* vol. 179-181, Part 1, pp. 425-428, 1991.

[7] M. Yamanouchi, M. Tamura, H. Hayakawa, A. Hishinuma, and T. Kondo, "Accumulation of engineering data for practical use of reduced activation ferritic steel: 8%Cr-2%W-0.2%V-0.04%Ta-Fe", *Journal of Nuclear Materials,* vol. 191-194, Part B, pp. 822-826, 1992.

[8] F. Abe, T. Noda, H. Araki, and S. Nakazawa, "Alloy composition selection for improving strength and toughness of reduced activation 9Cr-W steels", *journal of Nuclear Materials,* vol. 179-181, Part 1, pp. 663-666, 1991.

[9] L. F. Coffin, "The Influence of Mean Stress on the Mechanical Hysteresis Loop Shift of 1100 Aluminum", *Journal of Fluids Engineering,* vol. 86(4), pp. 673-680, 1964.

[10] G. Facheris and K. G. F. Janssens, "An internal variable dependent constitutive cyclic plastic material description including ratcheting calibrated for AISI 316L", *Computational Materials Science,* vol. 87, pp. 160-171, 2014.

[11] G. Facheris and K. G. F. Janssens, "Cyclic mechanical behavior of 316L: Uniaxial LCF and strain-controlled ratcheting tests", *Nuclear Engineering and Design,* vol. 257, pp. 100-108, 2013.

[12] Y. Dong, G. Kang, Y. Liu, H. Wang, and X. Cheng, "Dislocation evolution in 316L stainless steel during multiaxial ratchetting deformation", *Materials Characterization,* vol. 65, pp. 62-72, 2012.

[13] A. Sarkar, A. Nagesha, P. Parameswaran, R. Sandhya, and M. D. Mathew, "Influence of dynamic strain aging on the deformation behavior during ratcheting of a 316LN stainless steel", *Materials Science and Engineering: A,* vol. 564, pp. 359-368, 2013.

[14] S. Krishna, T. Hassan, I. Ben Naceur, K. Saï, and G. Cailletaud, "Macro versus micro-scale constitutive models in simulating proportional and nonproportional cyclic and ratcheting responses of stainless steel 304", *International Journal of Plasticity,* vol. 25, pp. 1910-1949, 2009.

[15] G. Kang, Q. Gao, and X. Yang, "Uniaxial and non-proportionally multiaxial ratcheting of SS304 stainless steel at room temperature: experiments and simulations", *International Journal of Non-Linear Mechanics,* vol. 39, pp. 843-857, 2004.

[16] G. Kang, Q. Gao, L. Cai, and Y. Sun, "Experimental study on uniaxial and nonproportionally multiaxial ratcheting of SS304 stainless steel at room and high temperatures", *Nuclear Engineering and Design,* vol. 216, pp. 13-26, 2002.

[17] Q. Gao, G. Z. Kang, and X. J. Yang, "Uniaxial ratcheting of SS304 stainless steel at high temperatures: visco-plastic constitutive model", *Theoretical and Applied Fracture Mechanics,* vol. 40, pp. 105-111, 2003.

[18] G. Kang, Y. Li, and Q. Gao, "Non-proportionally multiaxial ratcheting of cyclic hardening materials at elevated temperatures: Experiments and simulations", *Mechanics of Materials,* vol. 37, pp. 1101-1118, 2005.

[19] Y. Liu, G. Kang, and Q. Gao, "Stress-based fatigue failure models for uniaxial ratchetting–fatigue interaction", *International Journal of Fatigue,* vol. 30, pp. 1065-1073, 2008.

[20] G. Kang, Q. Gao, and X. Yang, "A visco–plastic constitutive model incorporated with cyclic hardening for uniaxial/multiaxial ratcheting of SS304 stainless steel at room temperature", *Mechanics of Materials,* vol. 34, pp. 521-531, 2002.

[21] G. Kang and Q. Kan, "Constitutive modeling for uniaxial time-dependent ratcheting of SS304 stainless steel", *Mechanics of Materials,* vol. 39, pp. 488-499, 2007.

[22] M. Shariati and H. Hatami, "Experimental study of SS304L cylindrical shell with/without cutout under cyclic axial loading", *Theoretical and Applied Fracture Mechanics,* vol. 58, pp. 35-43, 2012.

[23] C. K. Mukhopadhyay, T. Jayakumar, T. K. Haneef, S. Suresh Kumar, B. P. C. Rao, S. Goyal*, et al.*, "Use of acoustic emission and ultrasonic techniques for monitoring crack initiation/growth during ratcheting studies on 304LN stainless steel straight pipe", *International Journal of Pressure Vessels and Piping,* vol. 116, pp. 27-36, 2014.

[24] G.-H. Koo and J.-H. Lee, "Investigation of ratcheting characteristics of modified 9Cr–1Mo steel by using the Chaboche constitutive model", *International Journal of Pressure Vessels and Piping,* vol. 84, pp. 284-292, 2007.

[25] X.-T. Zheng, F.-Z. Xuan, and P. Zhao, "Ratcheting-creep interaction of advanced 9–12% chromium ferrite steel with anelastic effect", *International Journal of Fatigue,* vol. 33, pp. 1286-1291, 2011.

[26] M. Yaguchi, "Ratchetting of viscoplastic material with cyclic softening, part 1: experiments on modified 9Cr-1Mo steel", *International Journal of Plasticity,* vol. 21, pp. 43-65, 2005.

[27] P. Zhao and F.-Z. Xuan, "Ratchetting behavior of advanced 9–12% chromium ferrite steel under

creep-fatigue loadings", *Mechanics of Materials,* vol. 43, pp. 299-312, 2011.

[28] M. Ando, N. Isobe, K. Kikuchi, and Y. Enuma, "Effect of ratchet strain on fatigue and creep–fatigue strength of Mod.9Cr–1Mo steel", *Nuclear Engineering and Design,* vol. 247, pp. 66-75, 2012.

[29] Y. Li, X. Pan, and G. Wang, "Low cycle fatigue and ratcheting properties of steel 40Cr under stress controlled tests", *International Journal of Fatigue,* vol. 55, pp. 74-80, 2013.

[30] G. Kang, Y. Liu, J. Ding, and Q. Gao, "Uniaxial ratcheting and fatigue failure of tempered 42CrMo steel: Damage evolution and damage-coupled visco-plastic constitutive model", *International Journal of Plasticity,* vol. 25, pp. 838-860, 2009.

[31] G. Kang, Y. Liu, and J. Ding, "Multiaxial ratchetting–fatigue interactions of annealed and tempered 42CrMo steels: Experimental observations", *International Journal of Fatigue,* vol. 30, pp. 2104-2118, 2008.

[32] C. Li, G. Chen, X. Chen, and W. Zhang, "Ratcheting strain and simulation of 16MnR steel under uniaxial cyclic loading", *Computational Materials Science,* vol. 57, pp. 43-47, 2012.

[33] M. Zeinoddini and M. Peykanu, "Strain ratcheting of steel tubulars with a rectangular defect under axial cycling: A numerical modeling", *Journal of Constructional Steel Research,* vol. 67, pp. 1872-1883, 2011.

[34] G. Kang, Y. Dong, Y. Liu, H. Wang, and X. Cheng, "Uniaxial ratchetting of 20 carbon steel: Macroscopic and microscopic experimental observations", *Materials Science and Engineering: A,* vol. 528, pp. 5610-5620, 2011.

[35] Y. Dong, G. Kang, Y. Liu, and H. Jiang, "Multiaxial ratcheting of 20 carbon steel: Macroscopic experiments and microscopic observations", *Materials Characterization,* vol. 83, pp. 1-12, 2013.

[36] X. Yang, "Low cycle fatigue and cyclic stress ratcheting failure behavior of carbon steel 45 under uniaxial cyclic loading", *International Journal of Fatigue,* vol. 27, pp. 1124-1132, 2005.

[37] N. Khutia, P. P. Dey, S. K. Paul, and S. Tarafder, "Development of non Masing characteristic model for LCF and ratcheting fatigue simulation of SA333 C–Mn steel", *Mechanics of Materials,* vol. 65, pp. 88-102, 2013.

[38] S. K. Paul, "Effect of anisotropy on ratcheting: An experimental investigation on IFHS steel sheet", *Materials Science and Engineering: A,* vol. 538, pp. 349-355, 2012.

[39] M. Wen, H. Li, D. Yu, G. Chen, and X. Chen, "Uniaxial ratcheting behavior of Zircaloy-4 tubes at room temperature", *Materials & Design,* vol. 46, pp. 426-434, 2013.

[40] J. Peng, C.-Y. Zhou, Q. Dai, X.-H. He, and X. Yu, "Fatigue and ratcheting behaviors of CP-Ti at room temperature", *Materials Science and Engineering: A,* vol. 590, pp. 329-337, 2014.

[41] L.-x. Cai, Q.-y. Niu, S.-y. Qiu, and Y.-j. Liu, "Ratcheting Behavior of T225NG Titanium Alloy under Uniaxial Cyclic Stressing: Experiments and Modeling", *Chinese Journal of Aeronautics,* vol. 18, pp. 31-39, 2005.

[42] Q. Kan and G. Kang, "Constitutive model for uniaxial transformation ratchetting of super-elastic NiTi shape memory alloy at room temperature", *International Journal of Plasticity,* vol. 26, pp. 441-465, 2010.

[43] G. Kang, "Advances in transformation ratcheting and ratcheting-fatigue interaction of NiTi shape memory alloy", *Acta Mechanica Solida Sinica,* vol. 26, pp. 221-236, 2013.

[44] M. Kotoul, "Constitutive modeling of ratcheting of metal particulate-reinforced ceramic matrix composites", *materials Science and Engineering: A,* vol. 319-321, pp. 657-661, 2001.

[45] Z. Zhang and X. Chen, "Multiaxial ratcheting behavior of PTFE at room temperature", *Polymer*

Testing, vol. 28, pp. 288-295, 2009.

[46] A. D. Drozdov and J. d. Christiansen, "Cyclic viscoelastoplasticity of polypropylene/nanoclay hybrids", *Computational Materials Science,* vol. 53, pp. 396-408, 2012.

[47] M. Shariati, H. Hatami, H. Yarahmadi, and H. R. Eipakchi, "An experimental study on the ratcheting and fatigue behavior of polyacetal under uniaxial cyclic loading", *Materials & Design,* vol. 34, pp. 302-312, 2012.

[48] G. Tao and Z. Xia, "Ratcheting behavior of an epoxy polymer and its effect on fatigue life", *Polymer Testing,* vol. 26, pp. 451-460, 2007.

[49] M. Yaguchi and Y. Takahashi, "Ratchetting of viscoplastic material with cyclic softening, part 2: application of constitutive models", *International Journal of Plasticity,* vol. 21, pp. 835-860, 2005.

[50] K. Zhang and J. Aktaa, "Characterization and modeling of the ratcheting behavior of the ferritic–martensitic steel P91", *Journal of Nuclear Materials,* vol. 472, pp. 227-239, 2016.

[51] K. Zhang and J. Aktaa, "Ratcheting behavior of Eurofer97 at 550 °C", *Nuclear Materials and Energy,* vol. 15, pp. 97-102, 2018.

[52] A. Möslang, E. Diegele, M. Klimiankou, R. Lässer, R. Lindau, E. Lucon*, et al.*, "Towards reduced activation structural materials data for fusion DEMO reactors", *Nuclear Fusion,* vol. 45, pp. 649-655, 2005.

[53] A. A. Saad, W. Sun, T. H. Hyde, and D. W. J. Tanner, "Cyclic softening behaviour of a P91 steel under low cycle fatigue at high temperature", *Procedia Engineering,* vol. 10, pp. 1103-1108, 2011.

[54] J. Aktaa, M. Weick, and M. Walter, High Temperature Creep-Fatigue Structural Design Criteria for Fusion Components Built from EUROFER 97, Karlsruhe Institute for Technology FZKA 7309, 2007.

[55] F. Tavassoli, "Eurofer Steel, Development to Full Code Qualification", *Procedia Engineering,* vol. 55, pp. 300-308, 2013.